Spatial and Temporal Variation of Precipitation in Greece and Surrounding Regions Based on Global Precipitation Climatology Project Data

N. HATZIANASTASSIOU, B. KATSOULIS, J. PNEVMATIKOS, AND V. ANTAKIS

Laboratory of Meteorology, Department of Physics, University of Ioannina, Ioannina, Greece

(Manuscript received 15 September 2006, in final form 16 July 2007)

ABSTRACT

In this study, the spatial and temporal distribution of precipitation in the broader Greek area is investigated for the 26-yr period 1979–2004 by using monthly mean satellite-based data, with complete spatial coverage, taken from the Global Precipitation Climatology Project (GPCP). The results show that there exists a clear contrast between the more rainy western Greek area (rainside) and the drier eastern one (rainshadow), whereas there is little precipitation over the islands, particularly in the southern parts. The computed long-term areal mean annual precipitation amount averaged for the study area is equal to $P = 639.8 \pm 44.8$ mm yr^{-1}, showing a decreasing trend of -2.32 mm yr^{-1} or -60.3 mm over the 26-yr study period, which corresponds to -9.4%. This decrease of precipitation, arising primarily in winter and secondarily in spring, is the result of a decreasing trend from 1979 through the 1980s, against an increase during the 1990s through the early 2000s, followed again by a decrease up to the year 2004. The performed analysis reveals an increasing trend of precipitation in the central and northern parts of the study region, contrary to an identified decreasing trend in the southern parts, which is indicative of threatening desertification processes in those areas in the context of climatic changes in the climatically sensitive Mediterranean basin. In addition, the analysis shows that the precipitation decrease is due to a corresponding decrease of maximum precipitation against rather unchanged minimum precipitation amounts. The analysis indicates that the changing precipitation patterns in the region during winter are significantly anticorrelated with the North Atlantic Oscillation (NAO) index values, against a positive correlation during summer, highlighting thus the role of large-scale circulation patterns for regional climates. The GPCP precipitation data are satisfactorily correlated with instrumental measurements from 36 stations uniformly distributed over the study area (correlation coefficient $R = 0.74$ for all stations; $R = 0.63$–0.91 for individual stations).

1. Introduction

Precipitation is one of the most important climatic variables playing a key role in the global energy and water cycle. Precipitation information is critical for understanding the hydrological balance and the complex interactions among the small- and large-scale components within the hydrological cycle. The latent heat associated with precipitation is a primary atmospheric energy source; the spatial and temporal distribution of precipitation is crucial for advancing our ability to model and predict weather and climate changes. The distribution of precipitation is also important for water management, agriculture, electrical power and flood control, and drought and flood monitoring on all spatial scales (Adler et al. 2003). A better understanding of the global and regional hydrological cycles is at the heart of the World Climate Research Programme (WCRP) and its key Global Energy and Water Cycle Experiment (GEWEX) component.

Precipitation is one of the parameters that is always considered in the discussions of present and future climatic changes. In those discussions, the Mediterranean basin (Greece included) is a very important area, since it is a climatically sensitive region, which is severely threatened by climatic changes, especially decreasing precipitation and desertification processes (Houghton et al. 2001). Change in precipitation and increase in evapotranspiration may lead to a reduction of the cultivated areas and more intensive farming, leading thus to a decrease in soil fertility. In the recent years, it is evident that the frequency, persistence, areal extent, and severity of long period dry conditions in the Medi-

Corresponding author address: Dr. Nikos Hatzianastassiou, Laboratory of Meteorology, Department of Physics, University of Ioannina, Ioannina 45110, Greece.
E-mail: nhatzian@cc.uoi.gr

DOI: 10.1175/2007JCLI1682.1

FIG. 1. The study region and the station locations (see also Table 1).

terranean countries have increased (e.g., Sahsamanoglou et al. 1992; Wigley 1992; Kutiel and Maheras 1996; Maheras et al. 1999; Houghton et al. 2001; Feidas and Lalas 2001; Anagnostopoulou et al. 2003).

For the investigation of recent climatic fluctuations in southern Europe and the Mediterranean, it is very important to know the precipitation pattern and distribution, and prediction, provided that the driving climatological factors (e.g., atmospheric circulation anomalies) are considered. It is therefore necessary to study the geographical and temporal distribution of precipitation for long periods. In southeastern Europe, Greece constitutes an interesting study region, due to its climate diversity, which is in turn attributed to its variable relief. The Greek peninsula with its islands of Aegean and Ionian Seas (Fig. 1) is located in the northeastern side of the Mediterranean basin separated from the vast North African deserts by the Mediterranean Sea. The orographic and topographic influences, along with the influence of the Mediterranean waters (warmer than the adjoining land in winter and cooler in summer), cause an uneven temporal and spatial distribution as well as variability of precipitation. Thus, an analysis of the precipitation regime could help the investigation in understanding the mechanisms which cause the peculiar precipitation variations in the vicinity of the Mideast and North African deserts. The precipitation regime in the broader Greek area has been studied in the past by various researchers (e.g., Karapiperis and Katsoulis 1969; Maheras 1981; Katsoulis and Kambezidis 1989; Maheras and Kolyva-Mahera 1990; Bloutsos 1993; Repapis et al. 1993; Amanatidis et al. 1997; Metaxas et al. 1999; Fotiadi et al. 1999; Nastos et al. 2002; Bartzokas et al. 2003; Tolika and Maheras 2005; Pnevmatikos and Katsoulis 2006, among others). All of these studies have been performed by using various statistical techniques, such as principal component or harmonic analysis. Nevertheless, all of these techniques have been performed by using precipitation measurements taken from surface stations distributed over the broader Greek region. This fact limits, at least partially, the validity of the derived conclusions as far as it concerns areas that are far enough from the stations' site. Thus, to ensure full spatial coverage, isohyets are most

often traced in between the stations, but this results in large uncertainties since precipitation is characterized by strong spatial variability, especially over areas with strong relief, such as Greece. In addition, there are errors resulting first from systematic measuring errors (rain gauge evaporation losses and drift of drops or snow particles by the wind) and second from incomplete observations (temporal gaps). Individual errors also emerge during the further data transmission and processing, for example, by typing, coding and decoding, or reformatting of the data (Rudolf and Schneider 2005). Therefore, gauge-observed data and interpolated gridded data fields do not represent the full truth. In contrast to surface precipitation measurements, satellite data are preferable since they are representative of an entire geographical area (cell). Moreover, they have the advantage of providing full spatial coverage of the study region. Of course, the satellite precipitation data also have their own problems and limitations and cannot represent the full truth by themselves, so that they need to be adjusted, validated, and verified against in situ observations (Rubel and Rudolf 2001).

During the last years, the rapid advance of satellite technology and remote sensing techniques made it possible to monitor precipitation from satellites. The Global Precipitation Climatology Project (GPCP) is the WCRP GEWEX project devoted to producing community analyses of global precipitation. It was established in 1986 (see Arkin and Xie 1994), and its primary goal is to provide a long time series of monthly mean precipitation data on 2.5° × 2.5° latitude–longitude grids by using satellite measurements in the infrared and microwaves combined with historical surface measurements. The primary product of GPCP is now available covering the whole time period from 1979 to 2004 (26 yr) and it provides the research community with precipitation information useful for a large number of applications both on global and regional scale. The GPCP is ideally suited for studying the spatial and temporal distribution of precipitation, the water cycle, and has the potential for detecting precipitation-based climate change signals on several temporal and spatial scales (Assessment of Global Precipitation, Gruber and Levizzani 2006; http://cics.umd.edu/~yin/GPCP/main.html). Of course there are a few limitations in the use of GPCP data, which have to be kept in mind when analyzing regional (but also global) trends of precipitation (e.g., Adler et al. 2003). These limitations are mainly associated with the fact that the record is inhomogeneous in terms of its input datasets. This inhomogeneity arises from the desire for the longest record possible and the limited length of record of the various satellites and satellite types. Therefore, there are differences in satellite orbital characteristics, fields of view, spatial sampling, pixel size, and temporal sampling for the various satellite systems that feed into the GPCP data, as well as changes in satellite sensors and in sensor characteristics as the instruments aged. Also, there are some problems with GPCP precipitation over the ocean, especially over middle and high latitudes, as well as over polar land areas (Adler et al. 2003), and problems associated with the rain gauge network utilized in GPCP (Gruber and Levizzani 2006). The single largest potential source of instrument-related inconsistencies in the temporal record of precipitation estimates is associated with the lack of passive microwave (PMW) data for precipitation estimates before July 1987 (and for December 1987). Nevertheless, the inhomogeneity in the GPCP input datasets is minimized through calibrations (Adler et al. 2003; Gruber and Levizzani 2006), as explained in section 2a. Therefore, despite its limitations, the GPCP dataset is valuable for studying climate variability on several temporal and spatial scales, taking into account the systematic observation requirements (accuracy and long-term stability) for satellite-based products for climate [Global Climate Observing System (GCOS) 2006].

In this study we made use of 26-yr mean monthly satellite-based precipitation data from GPCP to investigate and reassess the precipitation regime and changes over the broader Greek region (eastern Mediterranean). The study region extends over 32.5° to 42.5°N and 17.5° to 30°E (Fig. 1). Since it is the first time that satellite data are systematically used for the study region, these were compared against climatological precipitation data from surface measurements taken from 36 stations uniformly distributed over the region. The purpose is to intercompare and evaluate the two types of data, given the problems associated with both of them, as explained above. This is important, since a reasonable agreement between GPCP precipitation data and station measurements secures the validity of the conclusions of this study, based on satellite data. The results of this paper may add further to our skill for long-range prediction of precipitation provided that the climatological driving factors for precipitation, such as large-scale circulation, humidity, or atmospheric cloud condensation nuclei, are also considered.

In section 2, we give a short description of the climatological satellite mean monthly data, and the ground-based data used for intercomparison. The geographical distributions of the computed seasonal and mean annual precipitation climatologies are shown and discussed in section 3, as well as the intra-annual and seasonal variations. In section 4, we show and discuss the

interannual variation, as well as the long-term trends of precipitation over the study region, and relate them to large-scale circulation patterns. Finally, in section 5 the satellite-based precipitation data are thoroughly compared against high-quality precipitation measurements within the study region, before the summary and conclusions in section 6.

2. The data used

a. GPCP precipitation data

The GPCP satellite precipitation data (Huffman et al. 1997) are a combined product basically from three individual sources: microwave and infrared (IR) satellite-derived precipitation estimates and rain gauge data. However, other sources of precipitation data are also utilized by GPCP, such as the Global Historical Climatology Network (GHCN)–Climate Anomaly Monitoring System (CAMS) gauge analysis, Television and Infrared Observation Satellite (TIROS) Operational Vertical Sounder (TOVS)-based estimates, and the outgoing longwave radiation (OLR) precipitation index (Adler et al. 2003). The general approach is to combine the precipitation information available from each source into a final merged product, taking advantage of the strengths of each data type (Huffman et al. 1997). The microwave estimates are based on Special Sensor Microwave Imager (SSM/I) data from the Defense Meteorological Satellite Program (DMSP, United States) satellites that fly in sun-synchronous low-earth orbits. The IR precipitation estimates are obtained primarily from geostationary satellites operated by the United States, Europe, and Japan and secondarily from polar-orbiting satellites. Additional precipitation estimates are obtained based on TOVS and OLR measurements (Adler et al. 2003). The gauge data are collected, quality controlled, and analyzed by the Global Precipitation Climatology Centre (GPCC) of the Deutcher Wetterdienst, to contribute to the analysis over land. More specifically, the rain gauge analyses are used to adjust the biases in the multisatellite analysis over land (see Janowiak et al. 2001). A complete description of the GPCP data, methodology, errors, and combination methods is given by Huffman et al. (1997) and Adler et al. (2003). In this study, the version 2 of the GPCP monthly analysis was used, which is an extension of version 1. Sampling errors of the GPCP products are of the order of 10%–15% (Gruber and Levizzani 2006) and they are estimated using different sampling strategies and comparison with Tropical Rainfall Measuring Mission (TRMM) Microwave Imager (TMI) sampling. The sampling error dominates the total error of the version 2 gauge product, especially for data-poor regions and where precipitation is highly variable. The GPCP products validate relatively well against standard and special gauge datasets. In general there is a decrease in accuracy as the precipitation becomes light, the environment becomes more polar, and/or the surface becomes icy or frozen. The originally taken monthly data were subsequently averaged into annual and 3-month seasonal means.

Precipitation data from rain gauges, for the period 1986 to 2004, were constructed by the GPCC operated by the German Weather Service. The GPCC uses a variant of the spherical-coordinate adaptation of Shepard's method (Willmott et al. 1985) to interpolate the data observed at gauge stations to regular grid points at a resolution of $0.5° \times 0.5°$. These regular points are then averaged to provide monthly precipitation totals at the final $2.5° \times 2.5°$ resolution. This methodology helps counteract the uneven distribution of gauges in the final gauge product. The GPCP uses the version 2 rain gauge "monitoring" product. A detailed description of the GPCC data processing and analysis system is given by Rudolf (1993). The version 2 rain gauge data have high accuracy (Huffman et al. 1997) and are based on about 6500–7000 rain gauge stations worldwide, mostly synoptic and monthly climate reports collected from the Global Telecommunications Network in real time, supplemented by other worldwide data collections, such as the *Monthly Climatic Data for the World*. Our analysis has shown that during the study period, the number of stations within the study region ranged from 0 to 10, approximately, depending on the year and the location within the region. The largest number of stations was encountered in the northern part, and especially in the northwestern part of the region, whereas the least numbered stations were found in the southern part. Over most parts of the study region, the number of stations used in GPCC is smaller than six, while there are areas with no stations at all.

The microwave precipitation estimates were derived from SSM/I measurements at four frequencies (19.35, 22.235, 37, and 85.5 GHz) with dual polarization on each frequency (except vertical alone at 22 GHz). The microwave brightness temperatures, observed from a spaceborne sensor, are dependent upon the emission from the earth's surface and modified by the intervening atmosphere, principally due to hydrometeors. The GPCP employs two SSM/I algorithms, one for ocean regions based on emission and the other for land areas based on scattering (see Huffman et al. 1997; Adler et al. 2003). The period from mid-1987 to 2004, except for December 1987, contains the SSM/I data that are used to calibrate the geosynchronous IR estimates, while the earlier period is dependent on the OLR data as the

main satellite input, resulting thus in an inhomogeneity of the GPCP input datasets. This inhomogeneity is minimized by calibrating the OLR technique during the later SSM/I period (Adler et al. 2003). The calibration procedures can be found in other works (Adler et al. 1994; Turk et al. 2000; Kidd et al. 2003; Joyce et al. 2004; Huffman et al. 2007). The performed comparisons of the zonal mean annual precipitation for the 1979–86 period to the 1988–2003 period (Gruber and Levizzani 2006, their Fig. 3.1b) suggest that the SSM/I data have greatest influence on the ocean estimates in the tropics and land estimates at mid- to high latitudes during the latter period. The 1988–2003 estimates show slightly larger values of precipitation in the convergence zones and slightly lower values over the land areas. Over land the introduction of the GHCN–CAMS data prior to 1988 may have also influenced the magnitude differences. Comparisons between the first 8 yr (1979–87) of the GPCP data not containing passive microwave SSM/I-based estimates of precipitation against the later period containing PMW estimates (Gruber and Levizzani 2006) revealed great similarities in the overall spatial distribution of precipitation. Apart from regions influenced by El Niño–Southern Oscillation (ENSO) large systematic differences were not found in precipitation patterns that might be attributed to the lack of PMW data in the first 8-yr period (differences tend to be less than 0.5 mm day^{-1}). Consequently, our study region is not among those affected by potential inhomogeneities caused by the GPCP input data. Therefore the obtained results, especially those of precipitation time series for the study area and specific subareas, are not influenced by the inhomogeneities, which are not considered in the relevant discussion (see section 4).

The global IR precipitation estimates are generated by merging precipitation data observed by cooperating geostationary satellites [the Geostationary Operational Environmental Satellite (GOES), United States; the Geostationary Meteorological Satellite (GMS) Japan; and the Meteorological Satellite (Meteosat) European Union] at the Climate Prediction Center using the GOES Precipitation Index (GPI; Arkin and Meisner 1987) technique. Geostationary data consist in accumulated 3-hourly imagery. In cases where geostationary data are unavailable, the National Oceanic and Atmospheric Administration (NOAA) polar-orbiting satellites are used providing 0–4 images per day.

b. Surface measurements

The surface-based precipitation data were used in this study in terms of intercomparison with the GPCP data. They were obtained by the Hellenic National Meteorological Service (HNMS), the National Observatory of Athens (NOA), and the Aristotelian University of Thessaloniki (AUTH) stations, providing complete series of reliable data records. The available historical data consisted of monthly precipitation for 36 weather stations with homogenized records stretching as far back as 1900, with periods varying from station to station between 31 and 100 yr. Nevertheless, this study is restricted to the analysis of post-1979 data to overlap with the satellite-based data (the years for which both series are available). The stations were selected in a way to provide representation of the different climatic entities and rainfall regimes in Greece. Another criterion was that none of the selected stations moved to more than 1 km away from its original location. Table 1 lists the stations used, their geographical characteristics, and the period of precipitation measurements,

TABLE 1. The Greek stations and the period of precipitation measurements (months in parentheses).

	Station	Lat (°)(′)	Lon (°)(′)	Altitude (m)	Years (Months)
1	Agrinio	38°37′N	21°23′E	25	1979–87 (99)
2	Alexandroupoli	40°51′N	25°56′E	3.5	1979–99 (238)
3	Argostoli	38°11′N	20°29′E	22	1979–85 (73)
4	Arta	39°10′N	20°59′E	39	1979–87 (102)
5	Athens	37°58′N	23°46′E	107	1979–99 (221)
6	Hania	35°30′N	24°2′E	62	1979–99 (178)
7	Hios	38°31′N	26°9′E	4	1979–98 (152)
8	Heraklion	35°20′N	25°11′E	39.3	1979–99 (190)
9	Ioannina	39°40′N	20°51′E	484	1979–99 (243)
10	Kalamata	37°4′N	22°6′E	11	1979–91 (135)
11	Karpathos	35°30′N	27°13′E	8	1979–98 (149)
12	Kerkyra	39°37′N	19°55′E	4	1979–99 (236)
13	Korinthos	37°56′N	22°57′E	14.4	1979–83 (49)
14	Kozani	40°17′N	21°47′E	625	1979–99 (238)
15	Kithira	36°8′N	23°1′E	166	1979–97 (169)
16	Lamia	38°51′N	22°24′E	17.4	1979–97 (218)
17	Larissa	39°39′N	22°26′E	73.6	1979–99 (243)
18	Lefkada	38°50′N	20°43′E	1	1979–92 (152)
19	Lidoriki	38°31′N	22°8′E	600	1979–93 (173)
20	Limnos	39°53′N	25°4′E	12	1979–99 (227)
21	Methoni	36°50′N	21°42′E	33	1979–99 (210)
22	Milos	36°44′N	24°26′E	164	1979–98 (167)
23	Mitilini	39°4′N	26°36′E	4.2	1979–98 (188)
24	Naxos	37°6′N	25°23′E	9.8	1979–99 (176)
25	Patra	38°15′N	21°44′E	1	1979–99 (189)
26	Preveza	38°58′N	20°46′E	2	1979–85 (74)
27	Rodos	36°24′N	28°5′E	34.7	1979–98 (170)
28	Samos	37°42′N	26°55′E	2.3	1979–98 (180)
29	Skiros	38°54′N	24°33′E	4.6	1979–98 (196)
30	Soufli	41°7′N	26°11′E	21	1979–99 (239)
31	Sparti	37°4′N	22°25′E	212	1979–96 (164)
32	Siros	37°27′N	24°57′E	9.6	1979–98 (68)
33	Thessaloniki	40°37′N	22°57′E	40	1979–99 (249)
34	Trikala	39°33′N	21°46′E	110.2	1979–98 (226)
35	Tripoli	37°31′N	22°24′E	652.4	1979–85 (82)
36	Zakinthos	37°47′N	20°54′E	3	1979–97 (183)

whereas Fig. 1 shows the geographical distribution of the stations in the study region. The utilized stations' data were subjected to various tests and have been corrected for single- or multiple-step changepoints that may exist in the time series, incompleteness of records, and nonhomogeneity of data (for details see Pnevmatikos and Katsoulis 2006); therefore, they represent the most complete and fully analyzed surface measurements ever existed for the study region.

3. Precipitation climatology

a. Geographical distributions

The geographical distribution of GPCP seasonal precipitation (3-month totals) in the study region is given in Figs. 2a,c,e,g, averaged over the 26-yr period (1979–2004). In winter (Fig. 2a), that is, when the area is dominated by eastward-moving cyclones originating from intense cyclogenesis in northern Italy (Furlan 1977), the maximum precipitation values ($P \cong 300$–400 mm) occur in the rainside part of the region, that is, in western Greece, eastward of Rodos Island, and in the eastern Aegean Sea. In the windward districts of the relief, an orographic uplift takes the place of air masses having traveled above sea areas (Adriatic and Ionian Seas), leading thus to formation of precipitation. On the contrary, the rainshadow parts of eastern Greece and central Aegean Sea are characterized by lower precipitation amounts (≅250 mm), whereas the southern areas (south of Crete) have the minimum precipitation (≅100 mm). In spring (Fig. 2c), the regime of precipitation is slightly different, with maximum precipitation values in the northwestern part of the region, gradually decreasing from west to east and from north to south (≅60 mm). During summer (Fig. 2e), the precipitation values reach 120 mm in the north, being attributed to thermal convective storms and representing up to about 20% of the annual precipitation amounts, while in the southern part of the region the values are very small (17–60 mm). The small summer precipitation amounts are due to the Azores high extended in northerly directions and deflecting the tracks of depressions. In autumn (Fig. 2g), large precipitation amounts (≅300 mm), even larger than those in spring, fall in the western part of the study region. The spring and autumn precipitation amounts are due to depressions entering and/or developing in the Mediterranean basin as the Azores high retreats to southwesterly positions, or to combinations of these depressions with disturbances originating in central Europe. In general, the resulting precipitation regime, apart from synoptic- and mesoscale patterns, is also affected by the alteration of the flow field and thermodynamic structure, water–land contrasts, and mountainous and hilly terrain, being thus strongly variable. In general, the main features of the GPCP precipitation are in general qualitative agreement, with previous results by other works based solely on station measurements, though there are some differences both qualitative and quantitative.

Figure 2 also provides an insight on the temporal variability of precipitation, since the climatological mean patterns are not enough to describe the distribution of precipitation by themselves. Thus, the coefficient of variation (c_v) of precipitation is given in Figs. 2b,d,f,h, for each season, which was computed according to the formula

$$c_v = 100\frac{\sigma}{\overline{P}}, \tag{1}$$

where $\overline{P}$ is the 26-yr average precipitation and σ is the associated standard deviation (std dev; not shown here). The seasonal values of coefficients of variation range from about 20% to 40%, except for summer when they range from 30% to 65%. During winter, the largest variability is in the southeastern Aegean Sea and in the northern part of the study region, while the southwestern part has the smallest precipitation variability. During spring, there appears to be a north-to-south gradient, with smaller/larger variabilities in the north/south. In summer, there is generally small variability of precipitation in the study region, except from very large values in the sea southwest from Crete Island, corresponding, however, to small mean precipitation amounts.

Figure 3 shows the computed climatological mean annual precipitation based on GPCP data (1979–2004). On an annual mean basis, the northwestern part of the region and the islands of the north Ionian Sea receive the maximum precipitation amounts (972 mm), while the lowest precipitation falls in Crete and the Libyan Sea (304 mm). In general, the precipitation decreases from the western to the central and eastern parts of the mainland and to the Aegean Sea, whereas it increases again (up to 730 mm) in the islands of the eastern Aegean Sea and the western coasts of Asia Minor. In general, our results are in good qualitative agreement with previous studies with regard to the location of maximum and minimum precipitation in the study area (e.g., Karapiperis and Katsoulis 1969; Maheras and Kolyva-Mahera 1990; Flocas 1992; Fotiadi et al. 1999; Tolika and Maheras 2005, etc.). However, there are differences in precipitation amounts. For example, the previously reported amounts along the Pindus Mountain axis range up to 2000 mm (e.g., Flocas 1992; Fotiadi et al. 1999) against our values of about 1000 mm. These

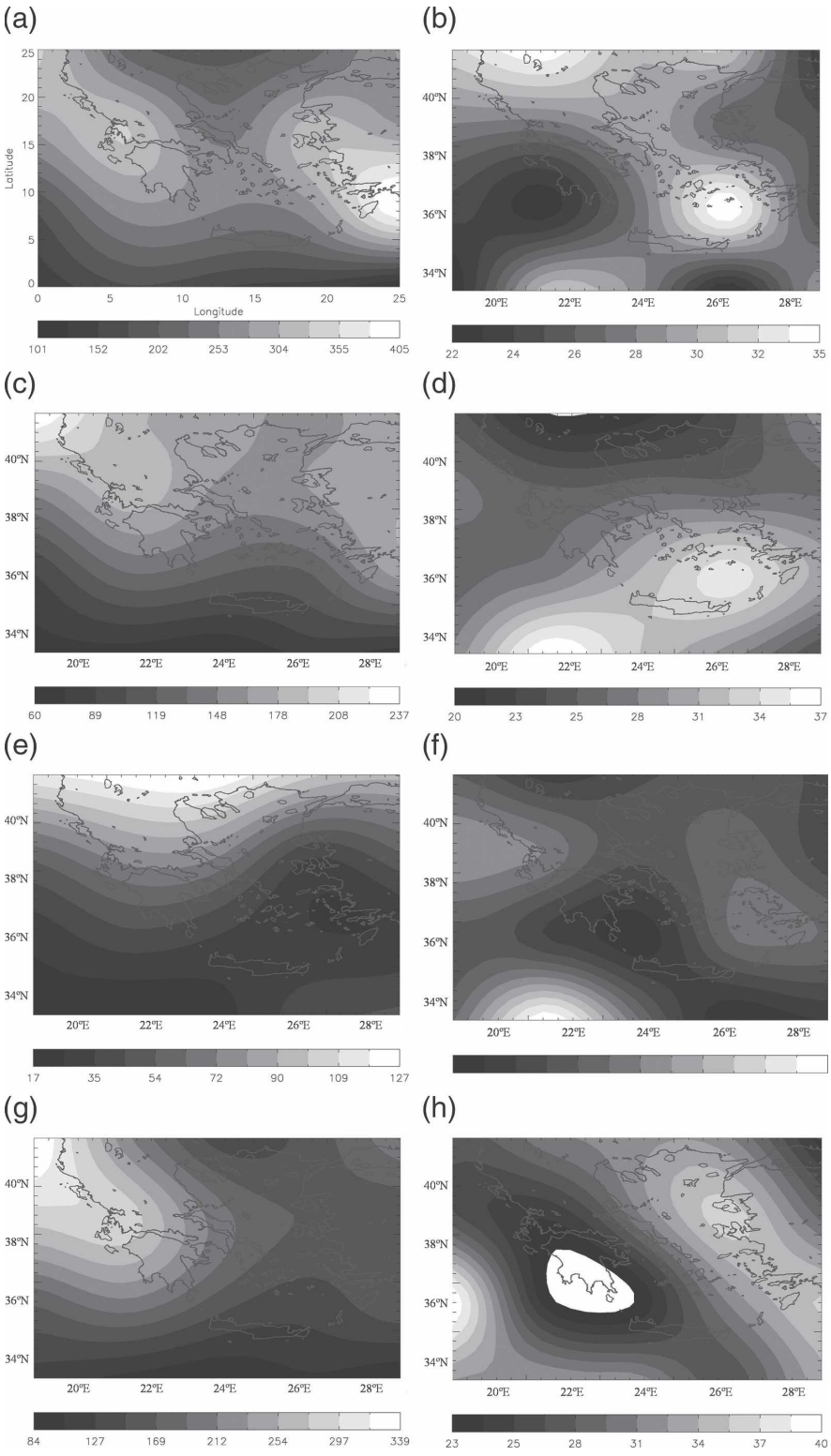

FIG. 2. Geographical distribution of 26-yr (1979–2004) average of precipitation (mm) and associated coefficients of variation over the region: (a),(b) winter, (c),(d) spring, (e),(f) summer, and (g),(h) autumn. (left) Means (%) and (right) coefficients of variation. Precipitation amounts were computed at 2.5° × 2.5° lat–lon resolution using GPCP data.

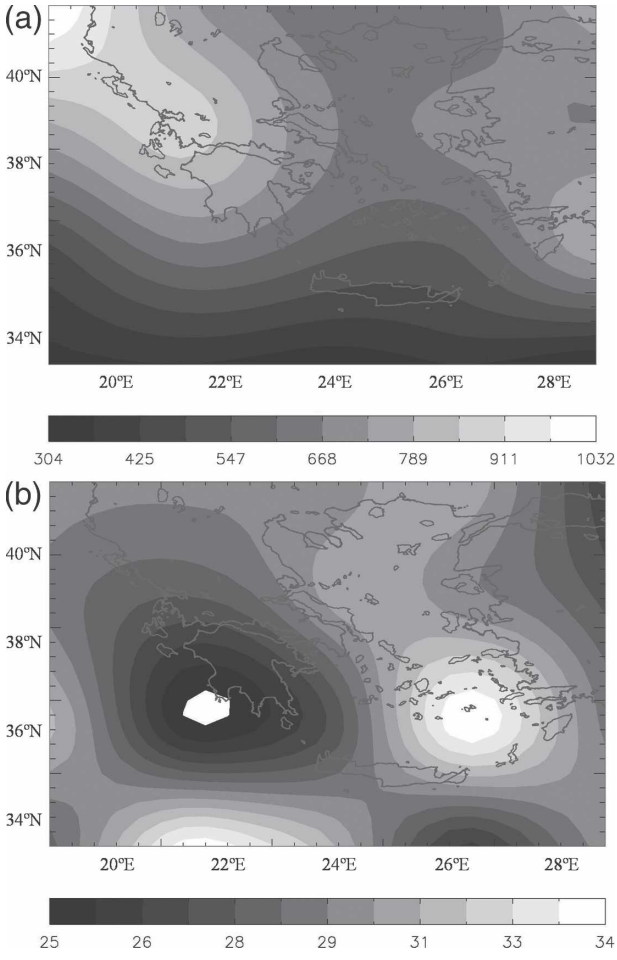

FIG. 3. Geographical distribution of 26-yr (1979–2004) average of GPCP precipitation (mm) at the surface of the region: (a) annual precipitation and (b) coefficient of variation (%) of annual precipitation.

differences are due to the fact that the previous estimates are based on local station measurements, against the representative regional averages of GPCP data. The minimum precipitation values (425–547 mm) in the southern Aegean Sea and Crete Island, based on GPCP, are quite smaller than the corresponding values of 500–600 mm reported recently by Pnevmatikos and Katsoulis (2006). These differences are explained by the different sources of data, as well as the different periods covered by the two sets of data. According to GPCP, the computed std dev of precipitation from its long-term mean (not shown here) ranges from 130 mm in Crete up to 260 mm in western Greece, approximately; these values correspond to about 25%–30% of the total absolute annual precipitation amounts. The computed c_v are shown in Fig. 3b, with values ranging from 25% to 35%. The largest variability of precipitation is found in the Aegean Sea and especially in its southeastern part, as well as southwest of Crete Island, whereas the smallest variability occurs in the southwest part of the Greek peninsula.

b. *Intra-annual variation of mean regional precipitation*

The spatial averages of the monthly mean precipitation were computed for the study region by averaging first along geographical longitude, then along latitude, by taking into account the surface area covered in each geographical cell (pixel). Most of the annual precipitation usually occurs in the winter months December to February, when the depression and frontal activity is quite frequent and intense over the region. Based on the GPCP data, the averaged precipitation over Greece and surrounding areas for the 26-yr period 1979–2004 (Fig. 4a) ranges from 17.8 mm in July (driest month) to 96.9 mm in December (wettest month), involving a significant annual amplitude of 79.1 mm. Note that the rate of precipitation of the wettest and driest months of the year is equal to 5.4, which is larger than the required value of 3 for the region's climate to be classified to the subtype "s" of the climatic type C according to Köppen's classification (Köppen 1918, 1936). Winter is the wettest season with 240.5 mm (contributing the 39.3% of the annual precipitation amounts), whereas summer is the driest one with only 58.8 mm (contributing 10% of the annual precipitation amount). The spring and autumn seasonal means are equal to 137.4 and 175.7 mm, respectively (contributions of 22.4% and 28.3%). The computed winter to summer precipitation rate for the whole region is equal to 4.1, clearly exceeding the value of 3, which is required (Palutikof et al. 1992; Palutikof and Wigley 1995) for the region to be classified in the Mediterranean climate type according to Köppen's classification. To show the large spatial variability of precipitation, even within a relatively small-scale region, such as Greece and the surrounding areas, in Fig. 4a are given the seasonal variations of GPCP precipitation for the pixels, including the stations of Thessaloniki (40°37′N, 22°57′E, northern station), Athens (37°58′N, 23°46′E, central station), Ioannina (39°40′N, 20°51′E, western station), Hios (38°31′N, 26°09′E, eastern station), and Heraklion (35°20′N, 25°11′E, southern station). Although a general agreement is found in terms of seasonal variability, that is, winter maximum and summer minimum values exist for all stations, there are, however, significant differences in terms of magnitude. Thus, the summer minimum values range between 7 and 30 mm (Heraklion and Thessaloniki, respectively), and the winter maxima range from 84 to 119 mm (Heraklion and Ioannina, respectively). There is also a slight difference in the seasonality between the

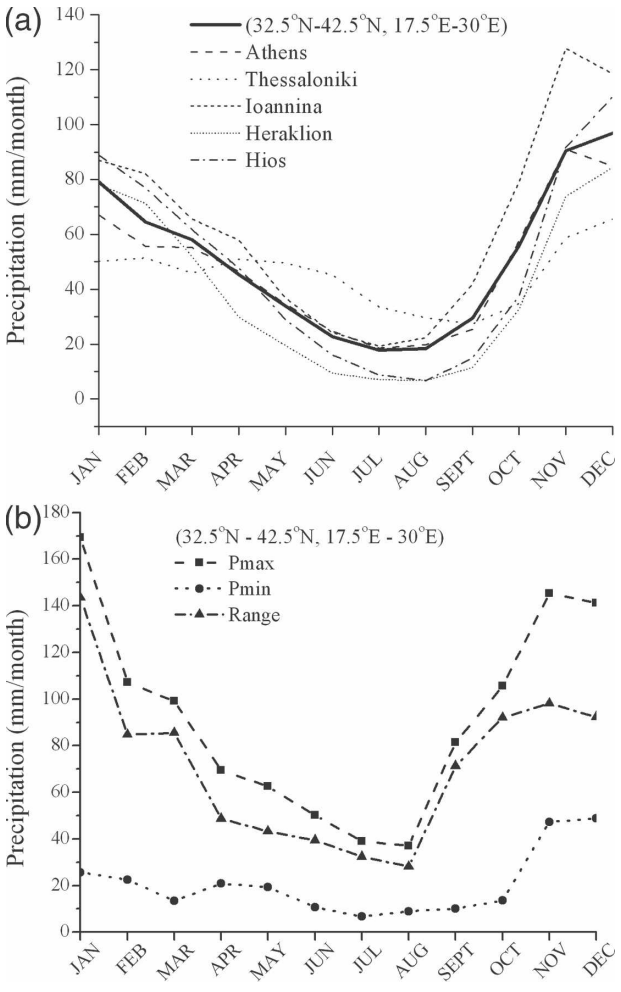

FIG. 4. Intra-annual variation of (a) long-term (1979–2004) GPCP precipitation (mm) averaged over the region (thick solid line) and for selected corners of the region; (b) maximum monthly precipitation (dashed line), minimum monthly precipitation (dotted line), and amplitude (maximum−minimum) of GPCP monthly precipitation (dashed–dotted line) averaged over the region (mm).

stations. Thus, despite the fact that the summer minimum for the whole region and most stations (e.g., Heraklion and Hios) occurs in August, for the western station of Ioannina it takes place in July, whereas for Thessaloniki it is delayed in September. Similarly, whereas the winter maximum precipitation is observed most often in December, for the central and western stations of Athens and Ioannina it takes place in November. Note that in autumn, winter, and spring, western Greece (Ioannina) receives the largest precipitation amounts, while the situation is different during summer, when the maximum precipitation falls in the north (e.g., Thessaloniki). In addition, it is very important to note the large disparity of the study region in its climate classification. Thus, despite the fact that the winter to summer rate of precipitation is equal to 4.1 for the whole region, there are large differences for specific subregions, since it varies from 1.5 for Thessaloniki (in the north) up to 7.1 for Heraklion (in the south). Beyond this, there are quite important differences between the different subregions in terms of contribution to the annual totals by summer and winter precipitation amounts. Thus, the contribution of summer to annual precipitation amount ranges from 4.9% for Heraklion up to 20% for Thessaloniki, while the winter contribution varies between 30.8% for Thessaloniki and 49.1% for Heraklion. The results of our precipitation analysis along with the regime of temperature indicate that the climate of the study region is classified to the type Csa according to Köppen's classification, whereas the types Cfa and Cfb also appear (e.g., in the northern Greek peninsula).

Apart from the intra-annual variation of long-term averaged precipitation for the study region, it is also important to examine the intra-annual variation of precipitation in terms of its monthly maximum and minimum values. These are the maximum and minimum precipitation values out of the total 26 corresponding values (for the 26 yr 1979–2004) for each month of the year. Thus, in Fig. 4b is given the intra-annual variation of the monthly maximum (P_{max}) and monthly minimum (P_{min}) precipitation for the study region, as well as the intra-annual variation of the amplitude of precipitation ($\Delta P = P_{max} - P_{min}$) for each month. There is a similar seasonal variability to that of long-term mean precipitation, but there are also some differences. However, even though the largest and smallest seasonal P_{max} values are found for winter and summer, respectively, the largest P_{max} values (≅170 mm) are not found in December as in Fig. 4a (i.e., for P) but in January. As far as it concerns the P_{min} values, these are consistently higher during winter (maximum in December with 48.8 mm) than in the rest of the year (10–20 mm). In general, the month by month variability is much larger for P_{max} than P_{min} values, so that the seasonal variability of the amplitude of precipitation ($\Delta P = P_{max} - P_{min}$ values) is largest in January (143.6 mm) and smallest in August (28.2 mm).

4. Time series of precipitation

a. Interannual variation and changes of regional means

The time series of deseasonalized mean monthly precipitation averaged over the study region is given in Fig. 5a, where the applied simple linear and multiple regression fits are also shown. The linear regression fit, ap-

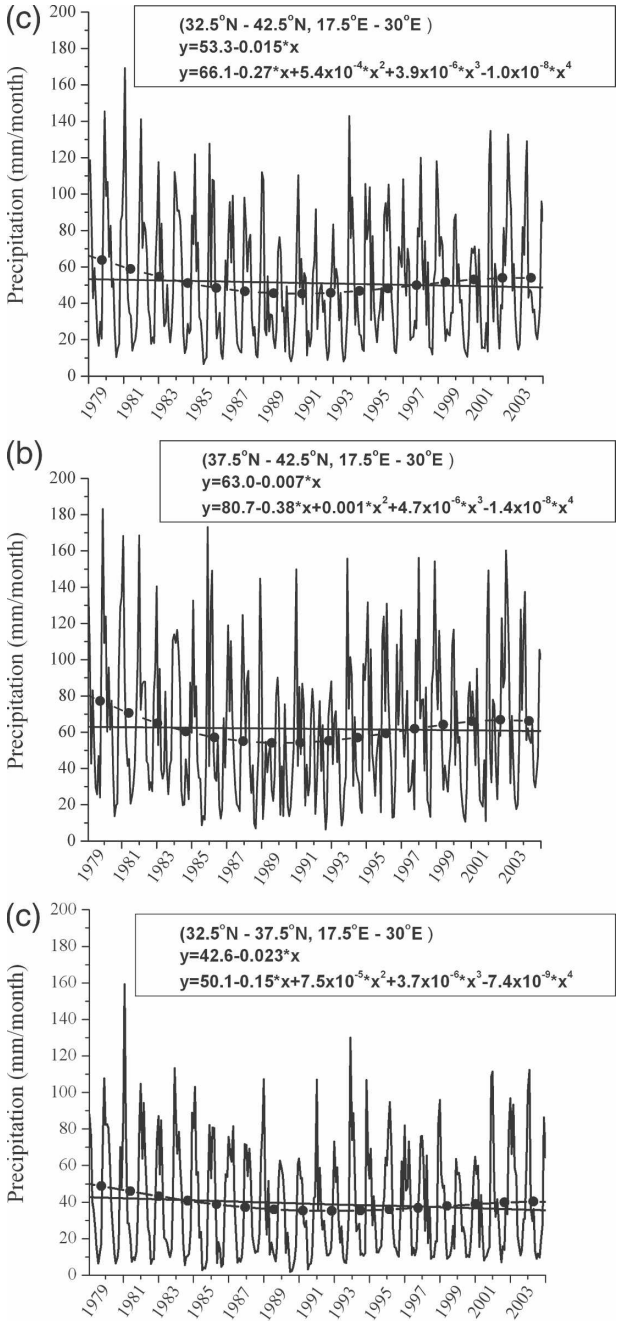

FIG. 5. Time series of GPCP precipitation (mm, solid lines) (a) averaged over Greece and surrounding areas, (b) averaged over northern areas, and (c) averaged over southern areas. Simple linear and fourth-order polynomial fits (dashed lines) are also displayed on the curves and the corresponding equations are given.

plied on the GPCP data, shows that the precipitation over the study area (areal mean equal to 53.3 ± 3.7 mm month^{-1}, equivalent to 639.8 ± 44.8 mm yr^{-1}) has not changed essentially during the 26-yr period, since a very small decrease in precipitation equal to −0.18 mm yr^{-1} is computed, which is not statistically significant (at the 95% confidence level) based on the applied Mann–Kendall test. However, this absence of any trend of precipitation for the study region is somehow misleading, because of the following reasons: (i) The application of a single linear regression fit over the study period possibly hides information appearing in shorter-term periods. Our analysis has shown that the fourth-order polynomial fit preserves features of the data, such as peak height and width, better than the method of linear averaging. Thus it was chosen as a compromise between simple linear fit and higher-order polynomial fits and complex smoothing methods. Indeed, the application of a fourth-order polynomial fit in Fig. 4a reveals that the precipitation over the study region has undergone modifications within the study period. More specifically, it has been decreasing from the late 1970s to the early 1990s, against an increasing trend persisting through the early 2000s. These two opposite tendencies result in the absence of a simple linear trend. (ii) The absence of any linear trend for the whole study region does not mean necessarily that any trend does not exist over specific subregions. To seek this, as a first step, the interannual variation of precipitation was computed separately for two large subregions, namely, the northern and southern districts of the entire study region. The northern subregion extends from 37.5° to 42.5°N and from 17.5° to 30°E, whereas the southern section covers the area from 32.5° to 37.5°N and from 17.5° to 30°E. The results for the two subregions, along with the applied linear regression and the fourth-order polynomial fits, are shown in Figs. 5b,c. According to our results, the precipitation over the northern sector of the study region (Fig. 5b) has decreased by 0.08 mm yr^{-1}, exhibiting first a decrease from 1979 through 1990 followed by an increase till 2004, similarly to what has happened for the whole study region. This decrease, which is equivalent to −2.08 mm over the 26-yr period, corresponds to a decrease of 3.3% (in relative terms) of the long-term mean precipitation for the northern sector. As far as it concerns the southern sector (Fig. 5c) the results are similar, so there is a decrease in the 1980s and an increase in the 1990s and early 2000s, resulting in a linear decreasing trend equal to −0.28 mm yr^{-1}, which is larger than that for the northern sector. This decrease is equal to −7.28 mm over the period 1979–2004, which corresponds to a decrease of the long-term mean precipitation for the southern sector equal to 17.1% (in relative terms). Nevertheless, none of the subregional trends was evaluated as statistically significant (at the 95% confidence level), based on the applied Mann–Kendall test. From these results, it is gathered that simply applying linear regression fits for extended geographical regions may not be adequate,

given that trends of different magnitude, or even of opposite sign, over smaller subregions may be combined resulting in hidden information about tendencies. On the contrary, it is more appropriate to apply linear regressions on a local scale, for example, at the pixel level, namely, for a geographical cell. This was also done and the results will be presented later (see Fig. 8, section 4b).

As far as it concerns the interannual variability of precipitation, it is found that on a mean monthly basis and for the whole region, it ranges roughly from 7 to 170 mm, always having maximum and minimum values in winter and summer, respectively. Apart from the primary maximum, which takes place either in December or January, there is often a secondary maximum occurring in the period from February to April. There exists an obvious year-to-year variability in precipitation, especially as far as it concerns the maximum values. From Figs. 5b,c, it is revealed that larger precipitation amounts fall in the northern part of the study region (ranging from 6.3 to 183.2 mm) than in the southern (1.9 to 159.3 mm) one. Beyond this finding, it is also worth noting that there are differences between the two subregions in terms of the years with absolute maximum precipitation. This finding highlights the different patterns in precipitation regime between the northern and southern parts of the study region in specific years, and they are attributed to different synoptic situations and/or orographic storms related to precipitation that affect different parts of a limited geographic area, such as Greece and the surrounding areas.

Apart from the interannual variation of the mean monthly precipitation averaged for the study region, it is also interesting to examine the interannual variation of the annual mean, maximum, and minimum precipitation in light of possible climatic changes. Thus, in Fig. 6a we display the year-to-year variation of the annual precipitation averaged for the entire study region. It is found that the annual precipitation ranges from 438 to 764 mm, so having a significant year-to-year variability. The applied linear regression fit reveals a decreasing trend equal to -2.32 mm yr^{-1}, which is equivalent to -60.3 mm over the 26-yr period (1979–2004). The p value for the t test of the slope $= 0$ is equal to 0.29. Based on our results, the areal mean averaged precipitation has decreased by 9.4% for the entire study region. Note that Pnevmatikos and Katsoulis (2006), using time series of precipitation data from the 36 stations utilized in this study, reported a decreasing trend during the second half of the twentieth century in the 92% of the studied stations. Furthermore, we applied here a fourth-order polynomial fit to GPCP precipitation time series to reveal smaller time-scale tendencies. The ob-

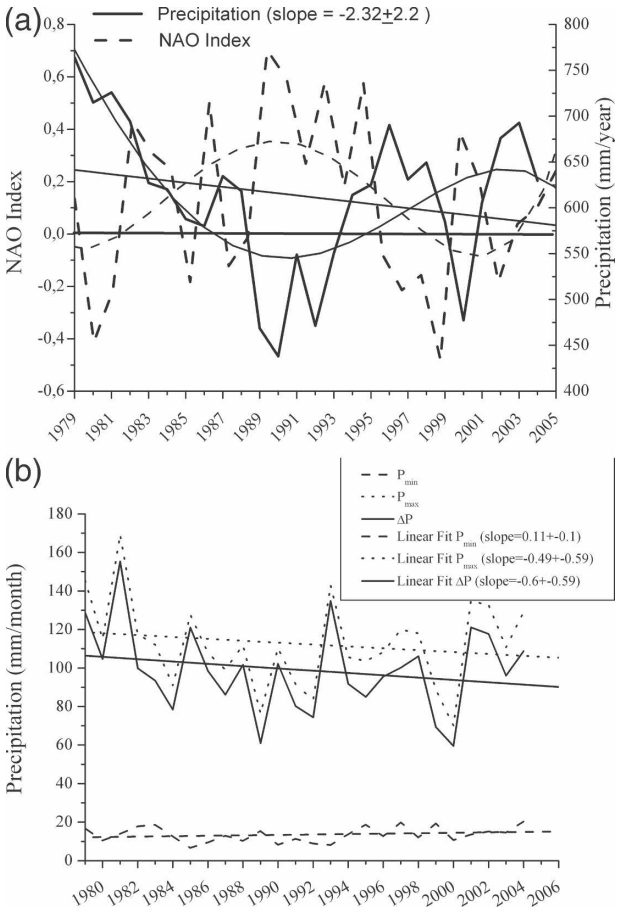

FIG. 6. Time series of (a) annual precipitation (mm) averaged over the region (solid lines) and annual NAOI (dashed lines), and (b) maximum monthly precipitation (dotted line), minimum monthly precipitation (dashed line), and annual amplitude of precipitation (maximum−minimum, solid line) as computed by using the GPCP dataset. Linear fits are also displayed on the curves and the corresponding slope values are given. In (a) the fourth-order polynomial fits for precipitation and NAOI are also displayed.

tained results show that first a decreasing trend of precipitation from 1979 through the end of the 1980s has occurred, while a subsequent increasing trend persisted from the early 1990s until the early 2000s. Hence, it seems that there is an approximate 10-yr cycle of precipitation, leading to an overall decrease during the 26-yr period 1979–2004. These periodicities may suggest some sun–weather relation, which deserves further investigation in the future. Nevertheless, the identified approximate 10-yr cycle of precipitation can be more directly related to the variability of the North Atlantic Oscillation (NAO), which varies from quasi-biennial to quasi-decadal and/or decadal time scales. It is well known that NAO, which is an atmospheric circulation pattern related to the surface pressure alternation between two large-scale dynamic centers of action so-

called the Azores high and the Icelandic low, controls weather and climate conditions and extremes in the Atlantic Ocean and the Mediterranean basin, including the study region.

To examine the relationship between precipitation variability in the study region and atmospheric circulation, we overlaid in Fig. 6a the year-to-year variation of the annual averages of NAO index (NAOI) values. The monthly mean values of NAOI were obtained by the Climate Prediction Center Web site (http://www.cpc.noaa.gov/products/precip/CWlink/pna/nao.shtml) of the National Centers for Environmental Prediction [(NCEP), National Oceanic and Atmospheric Administration (NOAA) National Weather Service]. There is a significant negative correlation of the NAOI with precipitation variability in Greece. Thus, during years with large/small NAOI values the precipitation over the study region is decreased/increased, respectively. The computed correlation coefficient (R) is equal to -0.58, and it is statistically significant (p value $= 0.0018$) at the 0.975 significance level. The applied fourth-order polynomial fit to NAOI values reveals an obvious anticorrelation between NAOI and precipitation over the study region. Thus, the decreasing precipitation from the late 1970s through the end of the 1980s is associated with an increase in NAOI, while the subsequent increasing trend of precipitation from the early 1990s until the early 2000s is associated with a corresponding decrease of NAOI. This link between regional precipitation variability and the NAO mode is very reasonable from a physical point of view and has been also reported by other investigators (e.g., Maheras et al. 1999; Quantrelli et al. 2001; Dünkeloh and Jacobeit 2003; Krichak and Alpert 2005; Feidas et al. 2007).

To further investigate the long-term changes of precipitation, we have computed and show in Fig. 6b the time series of regionally averaged monthly maximum and minimum precipitation per year ($P_{\max}$ and $P_{\min}$), as well as the series of the annual amplitude of precipitation ($\Delta P = P_{\max} - P_{\min}$). The monthly minimum precipitation does not exhibit a significant interannual variation, keeping almost steady values between 10 and 20 mm, and hence the applied linear regression fit indicates a very small increasing trend equal to 0.11 mm yr^{-1}; in other words, the monthly minimum precipitation per year has increased by 2.9 mm over the 26 yr. This change, which corresponds to a long-term mean monthly minimum precipitation of 13.54 ± 3.93 mm, is equivalent to a change of 21.4%, and it is not statistically significant at the 0.975 significance level according to the applied Mann–Kendall test (according to the t test, the p value is equal to 0.29). Moreover, our results indicate that during the period 1979–2004 the monthly maximum precipitation per year has decreased by 0.49 mm yr^{-1} or by 12.7 mm over the entire study period. This corresponds to a decrease of the long-term monthly maximum precipitation (112.43 ± 22.38 mm) equal to -11.3%, which is not statistically significant at the 0.975 significance level according to the applied Mann–Kendall test (the p value of the t test is equal to 0.41). Therefore, according to our analysis, the driest months of the year, that is, the summer months, have become slightly wetter (or less dry) during the course of 26 yr (1979–2004), while the wettest months, that is, the winter months, have become significantly drier (or less wet) for the study region. As a result, the annual amplitude of precipitation ΔP has linearly decreased by 0.6 mm yr^{-1} or by 15.6 mm over the 26 yr. This change is important compared to the long-term (26-yr mean) annual amplitude of precipitation, which is equal to 98.89 ± 22.42 mm, but it is not statistically significant according to both the Mann–Kendall and t tests at the 0.975 significance level (p value equal to 0.32). Wetter summer conditions for the study region combined with drier winter ones may be an indication of climate change and certainly need further investigation and analysis, which are planned for a future study. In addition, more detailed investigations are required focusing on precipitation trends similar to those presented in Fig. 6 but derived for each geographical cell in the study region.

To shed more light on the interannual variability of precipitation, we have also computed, and show in Fig. 7, the year-to-year variation of seasonal precipitation averaged for the study region. The seasonal variability is important since a situation is probable in which the annual mean precipitation does not exhibit an important change; but this may occur for specific seasons, producing counterbalancing trends. Hence, according to our analysis, the winter precipitation (Fig. 7a) shows a significant interannual variation, with values ranging from 141.1 to 363.9 mm. The applied linear fit indicates a decreasing 26-yr trend of winter precipitation equal to -1.95 ± 1.36 mm yr^{-1}; this is equivalent to a decrease of 50.7 mm over the period 1979–2004 and amounts to a decrease of the computed long-term winter precipitation value of 241.11 ± 53.04 mm equal to 21%. According to the applied Mann–Kendall test this trend is not statistically significant at the 0.975 significance level, but this is due to the small number of seasonal data. However, the p value of t test is equal to 0.16, indicating that the decreasing winter precipitation over the period 1979–2004 tends to be statistically significant. Note that Pnevmatikos and Katsoulis (2006) reported negative precipitation trends during winter in 33 out of 36 stations during the second half of the twenti-

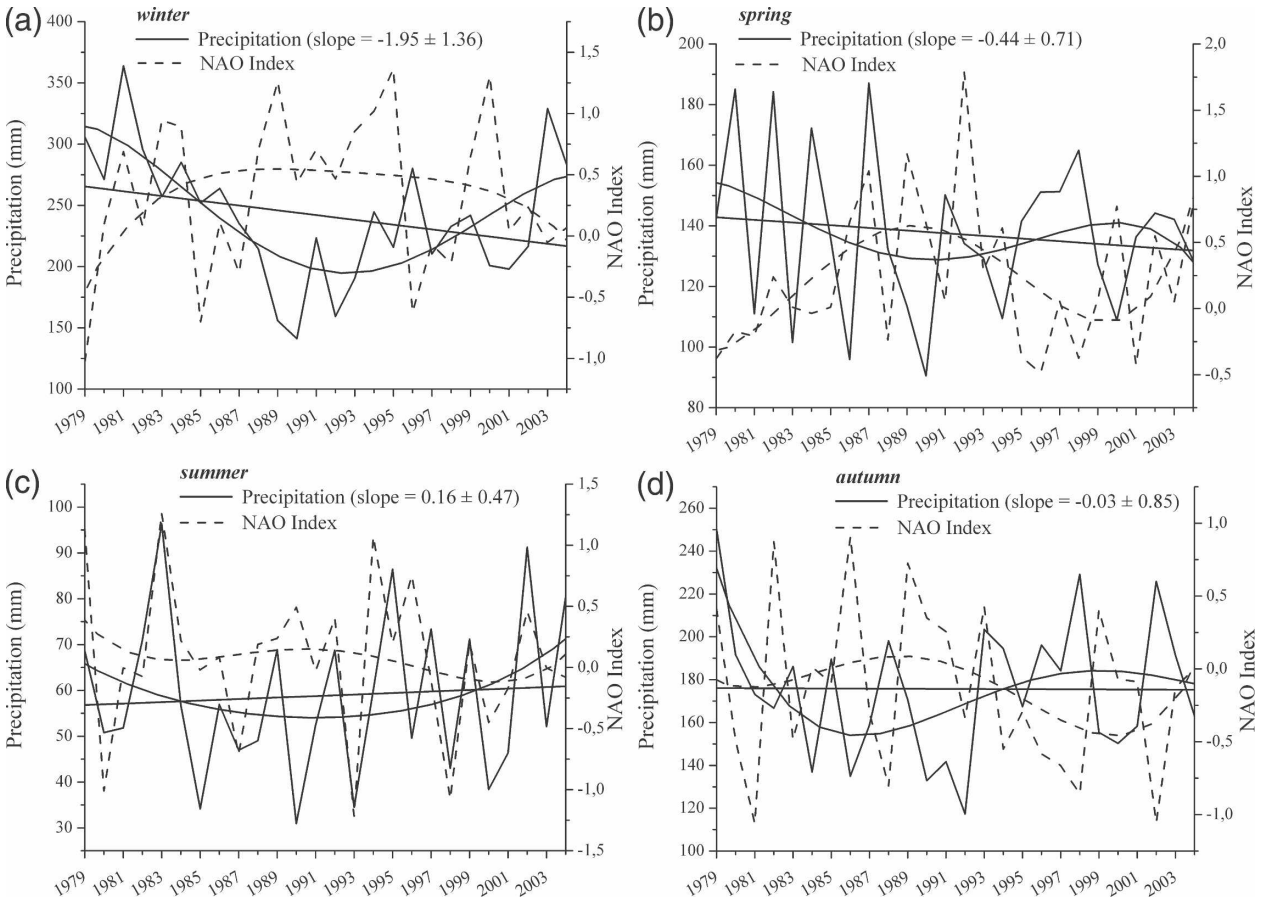

FIG. 7. Time series of seasonal precipitation (mm) averaged over the region, as computed from the GPCP dataset and NAOI values for (a) winter, (b) spring, (c) summer, and (d) autumn. Linear fits are also displayed on the precipitation curves along with the corresponding slope values, as well as fourth-order polynomial fits (solid lines), while fourth-order polynomial fits are also displayed for NAOI (dashed lines).

eth century, while Feidas et al. (2007) also reported decreasing trends in 22 stations over the period 1955–2001, in agreement with the findings by several researchers in the greater Mediterranean basin and surrounding areas (e.g., Sahsamanoglou et al. 1992). According to the applied fourth-order polynomial fit to the GPCP precipitation time series, the decrease of winter precipitation has taken place in the 1980s and 1990s, while from 2000 on, it seems to have increased again. The overplotted time series of seasonal averages of NAOI in Fig. 7a to those of precipitation for the period 1979–2004 confirms the findings from the corresponding annual time series (i.e., Fig. 6a). Thus, a negative correlation is found ($R = -0.36$), which is statistically significant at the 0.975 significance level (p value = 0.07). This connection between regional precipitation and NAOI, developed during winter, is expected and reasonable from a physical point of view and has been found and explained by many researchers (e.g., Hurrell 1995; Piervitali et al. 1997).

The summer precipitation values (Fig. 7c) vary between 31.0 and 96.3 mm and indicate a linearly increasing trend equal to 0.16 ± 0.47 mm yr^{-1} (or 4.16 mm over the 26-yr period), corresponding to an increase of 7.1% of the long-term summer precipitation value of 58.85 ± 17.68 mm. The long-term linearly increasing trend in summer precipitation resulted from a decrease through the late 1980s, surmounted by an increase since the early 1990s. It is interesting to note that the overplotted time series of mean summer NAOI values in Fig. 7c exhibit a significant positive correlation with the variability of regional mean precipitation (we have computed a correlation coefficient of $R = 0.5$, which is statistically significant at the 0.975 significance level, p value = 0.01). Thus, it is found that NAO has a significant influence on the precipitation regime in Greece not only in winter but also in summer, with an opposite correlation sign. This relationship can be explained by strengthened/weakened Azores high pressures over northern and central Europe combined with low/high

pressures over the Mediterranean basin during positive/negative values of the NAOI, resulting in more unstable/stable atmospheric conditions, respectively.

Examining the spring precipitation, there is an ascertained linearly decreasing trend equal to -0.44 ± 0.71 mm yr^{-1} (or -11.44 mm over the period 1979–2004), corresponding to a decrease of the long-term spring precipitation value of 137.37 ± 26.76 mm equal to 8.3%. This trend consists of decreasing tendencies from the year 1979 until the early 1990s and an increasing trend up to 2000. The spring averages of NAOI were not found to have a statistically significant correlation with the spring precipitation. As far as it concerns the autumn precipitation (Fig. 7d), it was found not to having undergone any change over the period 1979–2004; more specifically, it was found to have decreased by just 0.03 ± 0.85 mm yr^{-1} (or by only -0.78 mm over the period), which corresponds to a negligible decrease of the long-term autumn precipitation of 175.68 ± 31.86 mm by 0.44%. The applied fourth-order polynomial fit reveals that first there has been a significant precipitation decrease through the mid-1980s, followed by an increase up to 2000. There is a significant negative correlation between the mean autumn values of precipitation and NAOI (Fig. 7d). The computed correlation coefficient is equal to -0.37, and it is statistically significant (p value = 0.06) at the 0.975 significance level.

Note that none of the spring, summer, and autumn precipitation linear trends were evaluated as statistically significant according to the applied Mann–Kendall tests at the 0.975 significance level. Moreover, the p values of t test for spring, summer, and autumn are equal to 0.54, 0.73, and 0.97, respectively.

b. *Interannual variation and changes at geographical cell level*

In Fig. 8 is shown the computed trend of precipitation over the 26-yr period, based on the application of linear regression fit to the precipitation values for each geographical cell of the study region. It should be underlined that this precipitation trend is valuable because it is fully representative in terms of spatial coverage, contrary to surface-based instrumental measurements, which are simply point specific. It appears that the precipitation trend over the study region is not uniform, but there are two prevailing trends. Thus, it is ascertained that in the central and northern part of the studied region, the precipitation has increased by up to 0.4 mm yr^{-1}, or equivalently up to 10.7 mm, over the period 1979–2004. On the contrary, in the southern part of the region, and especially in the southern and southeastern Aegean Sea, the precipitation has decreased up to 0.7 mm yr^{-1}, or equivalently by up to 18.2 mm, over the study period. These modifications correspond to +1% and −5.7% of the climatological mean precipitation values for the regions in term. Our results are in line with the discussed enhancement of desertification processes threatening the southern part of the study region, and especially the island of Crete and south Peloponnese, where the devastating effects of desertification are already manifested in agriculture. Similar threatening desertification processes have also taken place in other Mediterranean regions, for example, Sicily, according to the Intergovernmental Panel on Climate Change (IPCC; Houghton et al. 2001). Note that Feidas et al. (2007) have reported decreasing precipitation trends over the whole Greek region, contrary to our results, but for the period 1955–2001, and solely based on 22 station measurements. The results of our study highlight the importance of detecting and analyzing any changing trends of climatic variables, and specifically of precipitation, to the highest possible spatial resolution, since it is clear that even for limited geographical regions, it is well possible to have opposite precipitation trends that can be hidden by averaging over space.

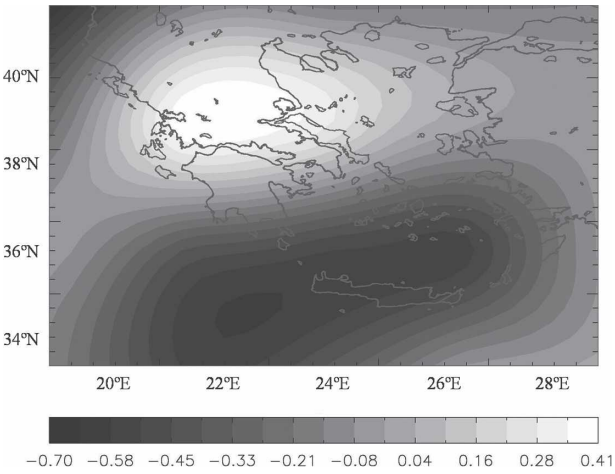

FIG. 8. Trends of precipitation (mm yr^{-1}) over the region resulting from the application of linear regression fits to the time series of monthly mean precipitation from the GPCP dataset.

c. *Discussion of interannual variation and changes of precipitation*

Our analysis of the 26-yr (1979–2004) GPCP precipitation data indicates an overall linearly decreasing trend in the annual precipitation over the study region. The application of a fourth-order polynomial fit reveals that this decrease resulted from a decreasing trend from the late 1970s to the early 1990s, against an increasing trend persisting through the early 2000s. These results

are in general agreement with the report of the IPCC (Houghton et al. 1996, 2001), indicating that annual precipitation trends in the twentieth century exhibit a decrease for southern Europe and the Mediterranean against a clear general increase for northern Europe, with the exception of Finland. They also agree with analyses (e.g., Maheras 1988; Amanatidis et al. 1993; Ben-Gai et al. 1994; De Luis et al. 2000; Lana and Burgueño 2000; Xoplaki et al. 2000; Gonzalez-Hidalgo et al. 2001; Piervitali et al. 1997, 1998; Esteban-Parra et al. 2003; Maheras and Anagnostopoulou 2003; Piervitali and Colacino 2003; Türkes 2003; Douguédroit and Norrant 2003; Norrant and Douguédroit 2003) that have been carried out for the study region or other Mediterranean areas, even though these have been conducted for individual stations and span earlier time periods than ours. Recently, Pnevmatikos and Katsoulis (2006), using monthly and annual rainfall data from the same 36 representative weather stations used in this study, reported that rainfall amounts began to decline in the 1980s, in agreement with the GPCP data. Besides, Feidas et al. (2007), using measurements of 22 surface stations in Greece for the period 1955–2001 and satellite data during the period 1980–2001, found that Greece, in general, presents a clear significant downward trend in annual precipitation for the period 1955–2001, beginning with the year 1984.

Our analysis has shown that the identified decreasing trend in precipitation over the period 1979–2004 is primarily due to a significant decrease of winter precipitation, and secondary to that of spring, against increasing summer precipitation amounts. These results are in agreement with the findings by other investigators for both western and eastern parts of the Mediterranean basin, indicating decreasing winter precipitation (e.g., Schönwiese et al. 1994; Palutikof et al. 1996; Piervitali et al. 1997; Schönwiese and Rapp 1997) or significantly decreasing precipitation during the last 20 yr of the period 1951–90 (e.g., Kadioglou 2000; Xoplaki et al. 2000). Two recent studies based on surface measurements from Greece (Pnevmatikos and Katsoulis 2006; Feidas et al. 2007) have reported a turnover of the decreasing precipitation trend during the 1990s, in agreement with our results. However, our results extending up to 2004 indicate that since the early 2000s the precipitation has been decreasing again.

The results of our analysis at the geographical cell level show that the overall decreasing trend in precipitation over the entire study region has mainly taken place in the southern part, as well as in the northwestern and northernmost extremes, against increasing tendencies identified for the central and northern part. These results are different than those given by previous studies (Feidas and Lalas 2001; Pnevmatikos and Katsoulis 2006; Feidas et al. 2007) who reported decreasing precipitation trends for the entire Greek territory and surrounding regions, with maximum negative trends in the northwestern Greek region and minimum trends in the eastern Greek region. The differences between our study and the others should be attributed to the different sources of data (satellite against station measurements) and the different study periods. For example, our results are based on GPCP satellite data covering the period 1979–2004, while those of Feidas et al. (2007) and Pnevmatikos and Katsoulis (2006) are based on 22 stations' surface measurements for the period 1955–2001 and 36 stations' surface measurements for the period 1950–1999, respectively.

5. Validation of satellite precipitation data

The reliability of GPCP data over the study region has been evaluated through extensive intercomparisons against best quality precipitation measurements taken from 36 HNMS stations within the study region (see section 2b). We note, however, that the surface-based measurements are point specific, while the GPCP satellite data are representative for a whole geographical cell with a surface area equal to about 280×280 km^2. This induces (expected) differences between the two sources of data, due to the strong spatial variability of precipitation, especially over regions with an intense and complex relief, such as the study region. It should also be noted that only a small part of the 36 stations (see section 2a) have been used in the GPCC. Therefore, a general qualitative agreement should be expected as a prerequisite for a successful comparison, rather than a very good or perfect quantitative agreement. Finally, note that the HNMS station data have been corrected for systematic gauge measuring errors. Under these conditions, the results of the comparison, which are presented in Fig. 9 for the total number of stations (36), are excellent. In Fig. 9 the GPCP data are compared to station measurements month by month and year by year giving a total number of 9072 data pairs corresponding to the sum of the months with available data for each station (indicated in the last column of Table 1). The value for each station is compared to the GPCP value of the geographical cell containing the location of the station. The correlation coefficient of the two series is $R = 0.745$ and is very satisfactory, whereas the standard deviation of differences, equal to 31.4 mm, and the bias between GPCP and station measurements, equal to -1.88 mm, are also very good. The correlation between the two series is statistically significant.

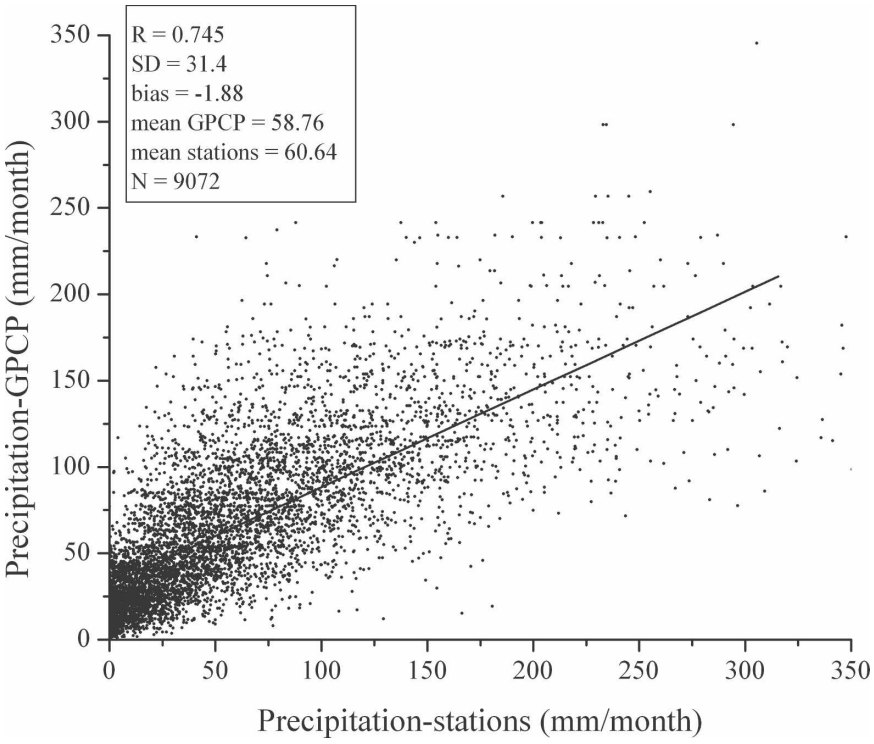

FIG. 9. Mean monthly precipitation (mm) at the surface of the region from data taken from the GPCP dataset vs data from 36 stations (refer to Table 1 and Fig. 1); R is the correlation coefficient, SD the std dev, and bias is the difference between the averaged value from GPCP and that from the stations.

A more detailed comparison of precipitation between GPCP data and HNMS station measurements is given in Table 2, where they are given the correlation coefficient, the standard deviation of differences, and the slope of the least squares line for each of the 36 stations. The comparison is performed for the common period of data for GPCP and HNMS stations, that is, for 1979–99. The significance level is equal to 0.975, and the p value is < 0.0001, that is, the results are statistically significant. In addition, the mean GPCP value and the bias between the GPCP and station values are also given. In general, the correlation coefficients are quite high, with values ranging from $R = 0.63$ to 0.91, whereas the standard deviations vary within the range std dev = 20.2–40.4 mm. The statistical significance of each individual correlation has been estimated using a standard Mann–Kendall test. As far as it concerns the bias values between GPCP and stations, they range from −32.6 (Samos) to 34.7 mm (Larissa). For a total number of 36 stations, the GPCP precipitation data are found to exceed the surface measurements in 23 stations, whereas they are smaller in 13 stations. It is interesting that all stations, except for Kozani and Patra, with GPCP data exceeding the surface measurements, are found in the eastern part of the study region. On the contrary, as far as it concerns the stations with underestimating GPCP data, these are not uniformly distributed since they are found in both the western (rainside) and eastern (rainshadow) parts of the region.

Figure 10 displays the comparison in terms of time series, between monthly mean GPCP precipitation data and corresponding ground measurements for eight selected HNMS stations representative for the eastern, western, northern, and southern parts of the study region. Intercomparisons of this type are helpful for detecting possible systematic differences or gradual increases/decreases in differences that can be attributed to problems associated with the instruments (both satellite and stations). Obviously, there is quite good agreement between satellite- and surface-based data both in terms of intra-annual and interannual variation, as well as in maximum and minimum values, without any indication of systematic large deviations. Beyond this, there is also a qualitative agreement between satellite and surface measurements in terms of long-term precipitation trends (for five out of eight stations), although the magnitude of trends is different. Such differences either in magnitude of precipitation amounts

TABLE 2. Validation of mean monthly GPCP satellite precipitation data at 2.5° × 2.5° lat–lon resolution against Greek stations with precipitation measurements in the study period (1979–99). The *R* and std dev values are from linear regression analysis between satellite and measured precipitation. Slope is the least squares line slope and its uncertainty (at the 95% significance level). They are also given the climatological (means 1979–99) precipitation amounts for each station, based on GPCP. Bias is the average difference between the satellite and the measured precipitation.

	Station	*R* (mm)	Std dev (mm)	Slope	Mean (mm)	Bias (mm)
1	Agrinio	0.85	28.9	−0.09 ± 0.17	72.12	−17.73
2	Alexandroupoli	0.81	20.2	−0.01 ± 0.03	52.84	9.05
3	Argostoli	0.91	22.2	−0.28 ± 0.25	72.12	−7.88
4	Arta	0.83	30.1	−0.09 ± 0.17	72.12	−17.96
5	Athens	0.82	22.1	0.01 ± 0.03	54.89	19.24
6	Hania	0.77	29.9	1.7 ± 0.10	47.83	−16.95
7	Hios	0.84	28.25	−0.01 ± 0.04	56.57	−10.41
8	Heraklion	0.84	23.8	−0.09 ± 0.03	45.69	−4.6
9	Ioannina	0.79	32.5	0.01 ± 0.04	72.11	−13.92
10	Kalamata	0.68	30.9	−0.07 ± 0.03	47.83	−28.73
11	Karpathos	0.77	28.6	−0.09 ± 0.03	45.69	−7.51
12	Kerkyra	0.85	28.07	0.01 ± 0.04	72.11	−14.54
13	Korinthos	0.73	27.46	0.01 ± 0.03	54.88	10.63
14	Kozani	0.7	23.84	−0.04 ± 0.03	60.87	22.07
15	Kithira	0.79	24.08	−0.07 ± 0.03	47.83	−9.47
16	Lamia	0.69	38.16	0.01 ± 0.04	72.11	22.89
17	Larissa	0.66	40.36	0.01 ± 0.04	72.11	34.71
18	Lefkada	0.88	23.75	0.01 ± 0.04	72.11	−14.67
19	Lidoriki	0.77	24.45	0.01 ± 0.03	54.88	−28.46
20	Limnos	0.79	32.02	−0.006 ± 0.04	56.57	15.47
21	Methoni	0.82	25.53	−0.06 ± 0.03	54.73	−10.47
22	Milos	0.73	26.51	−0.07 ± 0.03	47.83	−1.92
23	Mitilini	0.92	20.28	−0.006 ± 0.04	56.57	−8.5
24	Naxos	0.69	37.32	−0.006 ± 0.04	56.57	12.46
25	Patra	0.86	26.51	0.01 ± 0.04	72.11	15.24
26	Preveza	0.88	25.35	0.01 ± 0.04	72.11	−11.91
27	Rodos	0.77	37.8	−0.03 ± 0.05	63.02	−12.5
28	Samos	0.76	29	−0.09 ± 0.03	45.69	−32.6
29	Skiros	0.65	29.36	0.01 ± 0.03	54.88	19.71
30	Soufli	0.77	21.44	−0.01 ± 0.03	52.84	−8.95
31	Sparti	0.81	26.32	−0.06 ± 0.03	54.73	−18.98
32	Siros	0.63	26.41	−0.07 ± 0.03	47.83	4.98
33	Thessaloniki	0.66	21.24	−0.05 ± 0.02	51.56	15.1
34	Trikala	0.8	32	0.01 ± 0.04	72.11	7.04
35	Tripoli	0.88	23.75	−0.06 ± 0.03	54.73	−17.17
36	Zakinthos	0.84	23.67	−0.06 ± 0.03	54.73	−30.23

or in precipitation trends are more or less expected when attempting intercomparisons of this type between pixel (geographical cell) level satellite precipitation data and point-specific measurements, given the strong spatial variability of precipitation within a geographical area of 280 × 280 km^2. This is further strengthened in the case of stations whose location is significantly influenced by local meteorological and physicogeographical factors, for example, mountains with respect to their exposure to airflow. This characteristic is well illustrated by the differences found in measured precipitation amounts between stations that are located within the same geographical cell. For example, the central Greece stations of Larissa and Trikala have surface-measured climatological precipitation amounts equal to P = 37.41 and 65.08 mm, respectively, against a (pixel level) common GPCP value of 72.11 mm for the geographical cell in which they are both located. For the same reason, the GPCP-based precipitation is sometimes different than that from station measurements in winter, involving either an underestimation, for example, Ioannina, Heraklion, and Methoni (Figs. 8b,d,e, respectively), or overestimation, for example, Naxos and Larissa (Figs. 8f,h, respectively).

6. Summary and conclusions

Satellite-based data were used in this study to investigate the spatial and temporal distribution of precipitation in Greece and surrounding areas (32.5°–42.5°N

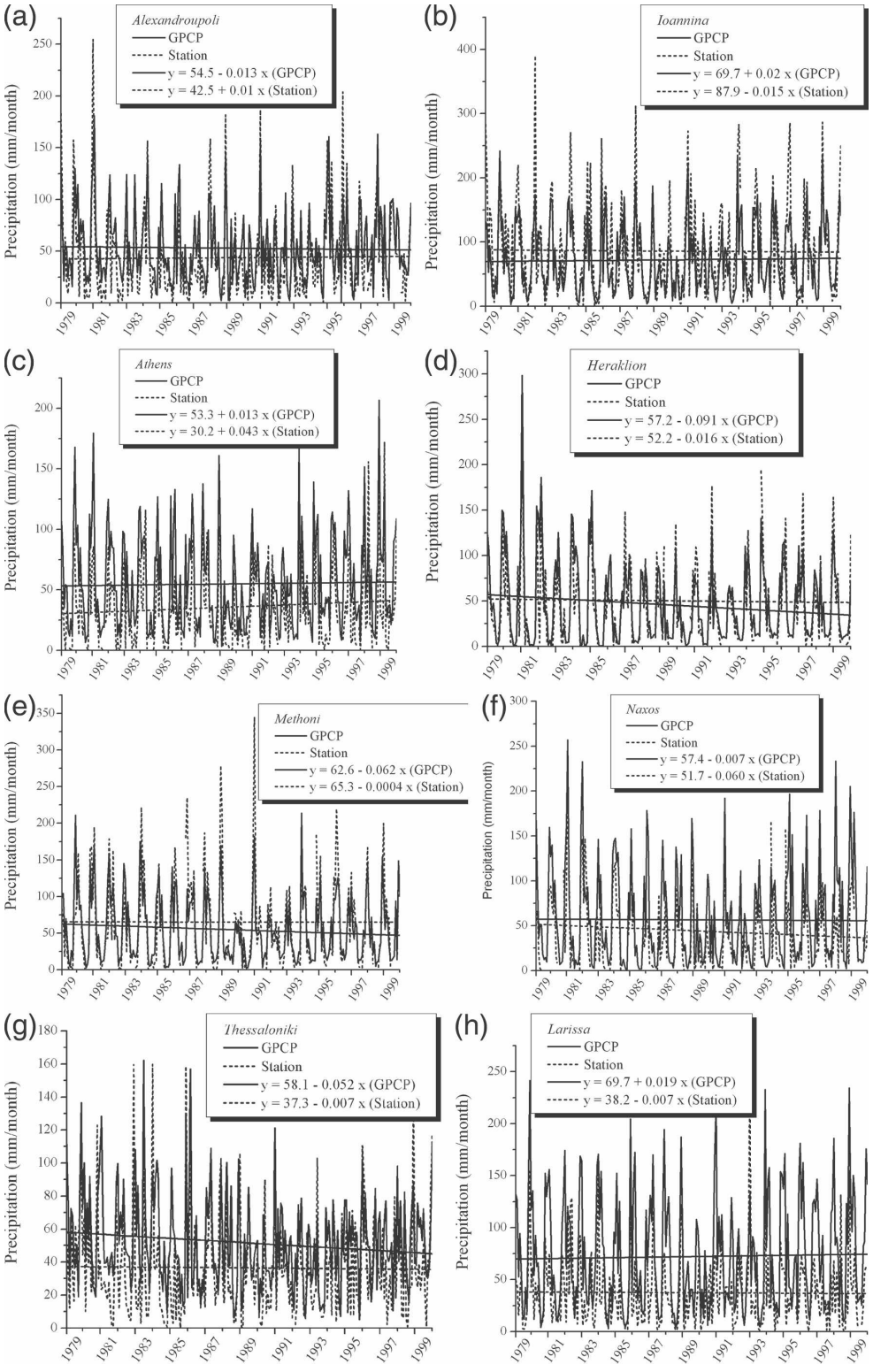

FIG. 10. Time series of mean monthly precipitation (mm) from the GPCP dataset (solid lines) and from ground measurements (dashed lines) at eight selected representative stations (refer to Table 1 and Fig. 1): (a) Alexandroupolis, (b) Ioannina, (c) Athens, (d) Heraklion, (e) Methoni, (f) Naxos, (g) Thessaloniki, and (h) Larissa. Linear fits are also displayed on the curves.

and 17.5°–30.0°E) on a mean monthly basis. Such studies are valuable for assessing the regional hydrological cycle and its variability in the context of possible climatic changes, especially for climatically sensitive regions, such as the Mediterranean basin since the study region is located within the basin's eastern part. Similar studies have been performed in the past, but they were solely based on station measurements that can hardly be representative of the spatial variability of precipitation, particularly for areas with a vertical and horizontal complex terrain. In this study, full spatial and long temporal coverage are ensured by using monthly precipitation data taken from the Global Precipitation Climatology Project (GPCP), along with measurements collected from 36 stations within the study region. The evaluation of GPCP precipitation data against those from stations shows a good agreement, with correlation coefficients between $R = 0.63$ and 0.91, scatter values ranging from about 20 to 40 mm, biases varying within 35 mm, and even 10–20 mm for most stations. The GPCP slightly underestimates (by 3.1%) the precipitation over the study region, in agreement with the reports from other studies (Nijssen et al. 2001) for regions with orographic features.

Overall, the averaged precipitation over Greece and surrounding areas for the study period (1979–2004) is equal to 639.8 mm [equivalent to 1.75 mm day^{-1} smaller than the global mean GPCP precipitation value of 2.61 mm day^{-1}, Gruber and Levizzani (2006)], showing a simple intra-annual variation, which also characterizes all subregions, with maximum values in winter (96.9 mm in December) and minimum in summer (17.8 mm in July). Nevertheless, there is a large spatial (both latitudinal and longitudinal) and temporal variability of precipitation, with amounts ranging from 17 to 406 mm, depending on the season and the subregion. The annual precipitation (P_a) amounts range from $P_a = 304 \pm 92$ mm in the southern marine part of the region to $P_a = 1033 \pm 316$ mm in the northwestern and western parts of the region, that is, in the rainside part, against values down to 670 ± 200 mm in the rainshadow, that is, in the eastern mainland, and down to 600 ± 180 mm in the central Aegean and northern mainland.

In this study, for the first time, the region has been objectively classified to the Mediterranean climate type according to Köppen's classification, based on regional averages of precipitation amounts ensuring complete spatial coverage; the computed winter to summer precipitation rate is equal to 4.1. However, for specific subregions this rate ranges from 1.5 in the north up to 7.1 in the south, underlining thus the large disparity of the region's climate.

The results of our study indicate a significant inter-annual variation of precipitation in the study region. The applied linear regression fit to the time series reveals a decreasing precipitation trend equal to -2.32 mm yr^{-1}, corresponding to an overall decrease of 60.3 mm over the study period, equivalent to -9.4%. This decrease, as shown by the applied fourth-order polynomial fit, results from a decrease of precipitation from the late 1970s through the early 1990s and a subsequent increase during the 1990s, followed again by a decrease persisting until the year 2004. The decrease in precipitation arises mainly from a decreasing trend during winter and secondarily in spring. The applied linear regression fits at the geographical cell level for the study region revealed decreasing precipitation trends in the southernmost part of Greece's mainland and in the southern and southeastern Aegean Sea, up to -5.1%, against increasing trends in the central and northern part of the region up to $+1\%$. These results indicate enhanced desertification processes in the south Peloponnese and Crete Island and highlight the existence of strong spatial contrasts in precipitation trends even in a limited geographical region; this is important and should be considered in the framework of the discussed climatic changes. The identified precipitation trends based on GPCP data are also supported by detected decreasing trends in most of the 36 stations examined in our study, whereas they seem to be in agreement with the results from other investigations, which are based on point-specific surface measurements. Our results also indicate that the annual amplitude of precipitation has decreased by 15.6 mm through the period 1979–2004, which is important compared to the corresponding absolute values ranging between 60 and 155 mm, approximately. These results are remarkable in view of possible climatic changes in this climatically sensitive region of the Mediterranean basin, but certainly they have to be analyzed and more thoroughly examined in the future. Our results verify that complete spatial averages of precipitation data, as those provided by GPCP, can be tentatively used to investigate possible changes of precipitation not only at global scale, but also on a regional basis (see, e.g., Gruber and Levizzani 2006).

The results of our analysis reveal a statistically significant correlation at the 0.975 level between the NAO index and the regional precipitation, on an annual basis. Moreover, they show an anticorrelation between NAOI and precipitation during winter and a positive correlation during summer, which are both statistically significant at the 0.975 significance level. In addition, negative correlations, but not statistically significant, were also identified during spring and autumn. Our re-

sults highlight the role of large-scale circulation patterns for the region's precipitation and its changes, which are related to climate change over southeastern Europe. Nevertheless, note that the detection of climate change at this space and time scale is rather difficult as the high variability in local climates can mask trends in the "noise" of natural fluctuations. Even though the identified trends in precipitation can be attributed to changes of atmospheric circulation (NAO), the extent of the variations is such that probably falls within the range of natural variability. Moreover, the relatively short period of data (1979–2004) makes difficult the identification of clear trends and creates uncertainty over the scale of natural variability. More extended remotely sensed precipitation data similar to those of GPCP [e.g., the Tropical Rainfall Measuring Mission (TRMM), the Program to Evaluate High Resolution Precipitation Products (PEHRPP), and the Global Precipitation Mission (GPM)], which are expected in the future, will be very helpful to improve the climatological assessments.

The decreasing trends in precipitation found in our study, apart from changing atmospheric circulation, may also be attributed to displacements of tracks of depressions. The study region's airmass regime is largely related to the passage of atmospheric disturbances (Katsoulis 1982). Thus it is likely that the identified precipitation changes are due to a general northward shift in atmospheric circulation patterns, which in turn influenced the paths and frequency of midlatitude depressions over the region. Nevertheless, no clear explanation can be given and more research is required to conclude the physical reasons for the precipitation changes.

The results of our analysis demonstrate the worth of using reliable climatological data from satellite-based programs, such as GPCP precipitation data, to reproduce the spatial and seasonal variation of precipitation for specific regions of the globe (Gruber and Levizzani 2006). Such regional distributions of precipitation are preferable and desirable since they provide complete spatial coverage, which is not secured by station measurements, and hence they are valuable for national policies related to water resources, especially for countries characterized by desertification threatened processes, such as Greece and the surrounding areas in the Mediterranean basin. They are also very important for the detection, assessment, and evaluation of possible effects of climatic changes.

Acknowledgments. The GPCP data were obtained from the GPCP Web site (http://cics.umd.edu/~yin/GPCP/main.html). The authors thank Dr. Emanuel Drakakis for his help in processing these data. The surface precipitation measurements were obtained from the Hellenic National Meteorological Service.

REFERENCES

Adler, R. F., G. J. Huffman, and P. R. Keehn, 1994: Global tropical rain estimates from microwave-adjusted geosynchronous IR data. *Remote Sensing Rev.,* **11,** 125–152.

——, and Coauthors, 2003: The Version-2 Global Precipitation Climatology Project (GPCP) Monthly Precipitation Analysis (1979–present). *J. Hydrometeor.,* **4,** 1147–1167.

Amanatidis, G. T., A. G. Paliatsos, C. C. Repapis, and J. G. Bartzis, 1993: Decreasing precipitation trend in the Marathon area, Greece. *Int. J. Climatol.,* **13,** 191–201.

——, C. C. Repapis, and A. G. Paliatsos, 1997: Precipitation trends and periodicities in Greece. *Int. J. Climatol.,* **16,** 191–201.

Anagnostopoulou, C., P. Maheras, T. Karacostas, and M. Vafiadis, 2003: Spatial and temporal analysis of dry spells in Greece. *Theor. Appl. Climatol.,* **74,** 77–91.

Arkin, P. A., and B. N. Meisner, 1987: The relationship between large-scale convective rainfall and cold cloud over the Western Hemisphere during 1982-84. *Mon. Wea. Rev.,* **115,** 51–74.

——, and P. Xie, 1994: The Global Precipitation Climatology Project: First Algorithm Intercomparison Project. *Bull. Amer. Meteor. Soc.,* **75,** 401–419.

Bartzokas, A., C. J. Lolis, and D. A. Metaxas, 2003: A study on the intra-annual variation and the spatial distribution of precipitation amount and duration over Greece on a 10-day basis. *Int. J. Climatol.,* **23,** 207–222.

Ben-Gai, T., A. Bitan, A. Manes, and P. Alpert, 1994: Long-term changes in annual rainfall patterns in southern Israel. *Theor. Appl. Climatol.,* **49,** 59–67.

Bloutsos, A., 1993: Harmonic analysis of the annual march of rainfall over Greece. *Proc. Geotechnical Chamber of Greece,* Thessaloniki, Greece, Geotechnical Chamber of Greece, 181–191.

De Luis, M., J. Raventos, J. C. Gonzalez-Hidalgo, J. R. Sanchez, and J. Cortina, 2000: Spatial analysis of rainfall trends in the region of Valencia (east Spain). *Int. J. Climatol.,* **20,** 1451–1469.

Douguédroit, A., and C. Norrant, 2003: Annual and century-scale trends of the precipitation in the Mediterranean area during the twentieth century. *Mediterranean Climate: Variability and Trends,* H.-J. Bölle, Ed., Springer, 159–163.

Dünkeloh, A., and J. Jacobeit, 2003: Circulation dynamics of Mediterranean precipitation variability 1948-98. *Int. J. Climatol.,* **23,** 1843–1866.

Esteban-Parra, M. J., D. Pozo-Vazquez, F. S. Rodrigo, and Y. Castro-Diez, 2003: Temperature and precipitation variability and trends in Northern Spain in the context of the Iberian peninsula climate. *Mediterranean Climate: Variability and Trends,* H.-J. Bölle, Ed., Springer, 259–276.

Feidas, H., and D. Lalas, 2001: Climatic changes in Mediterranean and Greece: A critical review. *Proc. Seventh Int. Conf. on Environmental Science and Technology,* Ermoupolis, Syros Island, Greece, University of the Aegean, 208–218.

——, C. Noulopoulou, T. Makrogiannis, and E. Bora-Senta, 2007: Trend analysis of precipitation time series in Greece and their relationship with circulation using surface and satellite data: 1955–2001. *Theor. Appl. Climatol.,* **87,** 155–177.

Flocas, A. A., 1992: *Lessons of Meteorology and Climatology* (in Greek). Ziti, 465 pp.

Fotiadi, A. K., D. A. Metaxas, and A. Bartzokas, 1999: A statistical study of precipitation in northwest Greece. *Int. J. Climatol.,* **19,** 1221–1232.

Furlan, D., 1977: The climate of southeast Europe. *The Climate of Central and Southern Europe,* C. C. Wallen, Ed., Vol. 6d, *World Survey of Climatology,* Elsevier, 185–235.

Global Climate Observing System (GCOS), 2006: Systematic observation requirements for satellite-based products for climate. GCOS-107, WMO/Tech. Doc. 1338, World Meteorological Organization and Intergovernmental Oceanographic Commission, 103 pp.

Gonzalez-Hidalgo, J. C., M. De Luis, J. Raventos, and J. R. Sanchez, 2001: Spatial distribution of rainfall trends in a western Mediterranean area. *Int. J. Climatol.,* **21,** 843–860.

Gruber, A., and V. Levizzani, 2006: Assessment of global precipitation: A project of the Global Energy and Water Cycle Experiment (GEWEX) Radiation Panel GEWEX, World Climate Research Programme, WMO. Assessment of Global Precipitation Climatology Project (GPCP), Executive Summary, 61 pp. [Available online at http://cics.umd.edu/~yin/GPCP/main.html.]

Houghton, J. T., L. G. Meira Filho, B. A. Callander, N. Harris, A. Kattenberg, and K. Maskell, 1996: *Climate Change 1995: The Science of Climate Change*. Cambridge University Press, 572 pp.

——, Y. Ding, D. J. Griggs, M. Noguer, P. J. van der Linden, X. Dai, K. Maskell, and C. A. Johnson, Eds., 2001: *Climate Change 2001: The Scientific Basis*. Cambridge University Press, 881 pp.

Huffman, G. J., and Coauthors, 1997: The Global Precipitation Climatology Project (GPCP) combined precipitation dataset. *Bull. Amer. Meteor. Soc.,* **78,** 5–20.

——, R. F. Adler, S. Curtis, D. T. Bolvin, and E. J. Nelkin, 2007: Global rainfall analyses at monthly and 3-hr time scales. *Measuring Precipitation from Space: EURAINSAT and the Future,* V. Levizzani, P. Bauer, and J. Turk, Eds., Springer Verlag, 291–306.

Hurrell, J. W., 1995: Decadal trends in the North Atlantic Oscillation: Regional temperatures and precipitation. *Science,* **269,** 676–679.

Janowiak, J. E., A. Gruber, S. Curtis, G. J. Huffman, R. F. Adler, and P. Xie, 2001: Evaluation and comparison of the CMAP and GPCP oceanic precipitation analyses. *Proc. WCRP/SCOR Workshop on Intercomparison and Validation of Ocean-Atmosphere Flux Fields,* WCRP-115, WMO/TD 1083, Washington, DC, 1–4.

Joyce, R. J., J. E. Janowiak, P. A. Arkin, and P. Xie, 2004: CMORPH: A method that produces global precipitation estimates from passive microwave and infrared data at high spatial and temporal resolution. *J. Hydrometeor.,* **5,** 487–503.

Kadioglou, M., 2000: Regional variability of seasonal precipitation over Turkey. *Int. J. Climatol.,* **20,** 1743–1760.

Karapiperis, L., and B. Katsoulis, 1969: Contribution to the study of rainfalls in some central and western parts of Greece (in Greek). *Mem. Nat. Obs. Athens,* **19,** 1–27.

Katsoulis, B. D., 1982: Climatic and synoptic considerations of the Mediterranean depressions developing and passing over or near the Balkan Peninsula. *Proc. First Hell-British Climatic Congress,* Athens, Greece, British Council, 73–84.

——, and H. D. Kambezidis, 1989: Analysis of the long-term precipitation series in Athens, Greece. *Climatic Change,* **14,** 263–290.

Kidd, C., D. R. Kniveton, M. C. Todd, and T. J. Bellerby, 2003: Satellite rainfall estimation using combined passive microwave and infrared algorithms. *J. Hydrometeor.,* **4,** 1088–1104.

Köppen, W. P., 1918: Klassification der klimate nach temperatur, nieduschlag und Jahreslanf. *Petermanns Geogr. Mitt.,* **64,** 193–203, 243–248.

——, 1936: Das geographische system der klimate. *Handbuch der Klimatologie,* W. Köppen and R. Geiger, Eds., IC.

Krichak, S. O., and P. Alpert, 2005: Signatures of the NAO in the atmospheric circulation during wet winter months over the Mediterranean region. *Theor. Appl. Climatol.,* **82,** 27–39.

Kutiel, H., and P. Maheras, 1996: Circulation and extreme rainfall conditions in the Eastern Mediterranean during the last century. *Int. J. Climatol.,* **16,** 73–92.

Lana, X., and A. Burgueño, 2000: Statistical distribution and spectral analysis of rainfall anomalies for Barcelona (NE Spain). *Theor. Appl. Climatol.,* **66,** 211–227.

Maheras, P., 1981: The precipitations variability over Aegean Sea. *Arch. Meteor. Geophys. Bioklimatol.,* **29,** 157–166.

——, 1988: Changes in precipitation conditions in the Western Mediterranean over the last century. *J. Climatol.,* **8,** 179–189.

——, and F. Kolyva-Mahera, 1990: Temporal and spatial characteristics of annual precipitation over the Balkans in the twentieth century. *Int. J. Climatol.,* **10,** 495–504.

——, and C. Anagnostopoulou, 2003: Circulation types and their influence on the interannual variability and precipitation changes in Greece. *Mediterranean Climate: Variability and Trends,* H.-J. Bölle, Ed., Springer, 215–239.

——, E. Xoplaki, and H. Kutiel, 1999: Wet and dry monthly anomalies across the Mediterranean basin and their relationship with circulation, 1860–1990. *Theor. Appl. Climatol.,* **64,** 189–199.

Metaxas, D. A., C. M. Philandras, P. T. Nastos, and C. C. Repapis, 1999: Variability of precipitation pattern in Greece during the year. *Fresenius Environ. Bull.,* **8,** 1–6.

Nastos, P. T., C. M. Philandras, and C. C. Repapis, 2002: Application of canonical analysis to air temperature and precipitation regimes over Greece. *Fresenius Environ. Bull.,* **11,** 488–493.

Nijssen, B., G. M. O'Donnell, D. P. Lettenmaier, D. Lohmann, and E. F. Wood, 2001: Predicting the discharge of global rivers. *J. Climate,* **14,** 3307–3323.

Norrant, C., and A. Douguédroit, 2003: Recent tendencies of precipitation and surface pressure in the Mediterranean basin (in French). *Ann. Géogr.,* **631,** 298–305.

Palutikof, J. P., and T. M. L. Wigley, 1995: Developing climate change scenarios for the Mediterranean region. *Climatic Change and the Mediterranean,* L. Jeftic, J. D. Milliman, and G. Sestini, Eds., Edward Arnold, 27–56.

——, X. Guo, T. M. L. Wigley, and J. M. Gregory, 1992: *Regional Changes in Climate in the Mediterranean Basin due to Global Greenhouse Gas Warming.* MAP Technical Reports Series 66, UNEP, 172 pp.

——, R. M. Trigo, and S. T. Adcock, 1996: Scenarios of future rainfall over the Mediterranean: Is the region drying? *Proc. Mediterranean Desertification, Research Results and Policy Implications,* Crete, Greece, Greek Diroctorate-General Research, 33–39.

Piervitali, E., and M. Colacino, 2003: Precipitation scenarios in the central-western Mediterranean Basin. *Mediterranean Cli-*

mate: Variability and Trends, H.-J. Bölle, Ed., Springer, 245–258.

——, ——, and M. Conte, 1997: Signals of climatic change in the Central-Western Mediterranean basin. *Theor. Appl. Climatol.,* **58,** 211–219.

——, ——, and ——, 1998: Rainfall over the central-western Mediterranean basin in the period 1951-1995. Part I: Precipitation trends. *Rev. Geophys. Space Phys.,* **21C,** 331–344.

Pnevmatikos, J. D., and B. D. Katsoulis, 2006: The changing rainfall regime in Greece and its impact on climatological means. *Meteor. Appl.,* **13,** 331–345.

Quantrelli, R., V. Pavan, and F. Molteni, 2001: Wintertime variability of the Mediterranean precipitation and its links with large-scale circulation anomalies. *Climate Dyn.,* **17,** 457–466.

Repapis, C. C., G. T. Amanatidis, A. G. Paliatsos, and H. Mantis, 1993: Spatial coherence of precipitation in Greece (in Greek). *Publ. Assoc. Int. Climatol.,* **6,** 333–340.

Rubel, F., and B. Rudolf, 2001: Global daily precipitation estimates proved over the European Alps. *Meteor. Z.,* **10,** 403–414.

Rudolf, B., 1993: Management and analysis of precipitation data on a routine basis. *Proc. Int. WMO/IAHS/ETH Symp. on Precipitation and Evaporation,* Bratislava, Slovakia, Slovak Hydrometeorological Institute, 69–76.

——, and U. Schneider, 2005: Calculation of gridded precipitation data for the global land-surface using in-situ gauge observations. *Proc. Second Workshop of the Int. Precipitation Working Group IPWG,* EUM P44, Monterey, CA, EUMETSAT, 231–247.

Sahsamanoglou, H. S., I. I. Makrogiannis, and Z. B. Rossidis, 1992: Characteristics of rainfall in the greater region of the Mediterranean. *Proc. First Panhellenic Conf. of Meteorology, Climatology and Physics of the Atmosphere,* Thessaloniki, Greece, Hellenic Meteorological Society, 147–153.

Schönwiese, C.-D., and J. Rapp, 1997: *Climate Trend Atlas on Europe—Based on Observations 1891–1990*. Springer, 240 pp.

——, ——, T. Fuchs, and M. Denhard, 1994: Observed climate trends in Europe 1891–1990. *Meteor. Z.,* **3,** 22–28.

Tolika, K., and P. Maheras, 2005: Spatial and temporal characteristics of wet spells in Greece. *Theor. Appl. Climatol.,* **81,** 71–85.

Turk, F. J., G. Rohaly, J. D. Hawkins, E. A. Smith, A. Grose, F. S. Marzano, A. Mugnai, and V. Levizzani, 2000: Analysis and assimilation of rainfall from blended SSM/I, TRMM, and geostationary satellite data. *Proc. 10th Conf. on Satellite Meteorology and Oceanography,* Long Beach, CA, Amer. Meteor. Soc., 66–69.

Türkes, M., 2003: Spatial and temporal variations in precipitation and aridity index series in Turkey. *Mediterranean Climate: Variability and Trends,* H.-J. Bölle, Ed., Springer, 181–213.

Wigley, T. M. L., 1992: Future climate of Mediterranean basin with particular emphasis on changes in precipitation. *Climatic Change and the Mediterranean,* L. Jeftic, J. D. Milliman, and G. Sestini, Eds., Edward Arnold, 15–44.

Willmott, C. J., C. M. Rowe, and W. D. Philpot, 1985: Small-scale climate maps: A sensitivity analysis of some common assumptions associated with grid-point interpolation and contouring. *Amer. Cartogr.,* **12,** 5–16.

Xoplaki, E., J. Luterbacher, R. Burkard, I. Patrikas, and P. Maheras, 2000: Connection between the large scale 500 hPa geopotential height fields and precipitation over Greece during wintertime. *Climate Res.,* **14,** 129–146.